

High-Pressure Flow Reactor Product Study of the Reactions of HO_x + NO₂: The Role of Vibrationally Excited Intermediates[†]

Timothy J. Dransfield,* Neil M. Donahue,[‡] and James G. Anderson

Department of Chemistry and Chemical Biology, Harvard University, Cambridge, Massachusetts

Received: July 5, 2000; In Final Form: October 18, 2000

The gas-phase reactions between HO_x and NO_x are critical in determining the chemical composition of both the troposphere and stratosphere. They dominate both interconversion among radical species and formation of stable reservoir species for both HO_x and NO_x. In many cases, the rates of these reactions are known, but the products and mechanisms are less well understood. In particular, the distribution of products among available channels as a function of temperature and pressure is very uncertain for several crucial reactions. One important reaction is that of OH with NO₂; some fraction of reactions may lead to an isomer of nitric acid, peroxyxynitrous acid (HOONO), though this species has not been observed in the gas phase. We present an investigation of that possibility. With reaction modulation FTIR spectroscopy in our high-pressure flow system, we are able to examine the behavior of various (HO_x + NO₂ → products) reactions with independent control over system temperature and pressure. Application of strict mass-balance in our wall-less reactor allows for quantitative analysis of reactant and product concentrations, even in those cases where the integrated bandwidths are unavailable. We examine the reactions HO₂ + NO₂ → HOONO₂ and OH + NO₂ → products. Each reaction proceeds through at least one vibrationally excited intermediate, and in each case there is a potential for the dynamics of those intermediates to produce unexpected behavior. In the case of HO₂ + NO₂, there is no evidence that a hydrogen atom transfer in the intermediate produces any HONO, even at low pressure. This is consistent with previous work. In the case of OH + NO₂, there are almost certainly two intermediates, HOONO and HONO₂, but we see no evidence for stable HOONO formation, even at 230 K.

Introduction

Our understanding of stratospheric ozone depletion is highly dependent on our understanding of the partitioning of nitrogen in the atmosphere. In particular, the reactions which lead to exchange between reactive nitrogen (NO_x), and the reservoir NO_y species are of critical importance. The reactions of HO_x with NO₂ are the dominant gas-phase source of NO_y, sequestering NO_x and HO_x in long-lived, relatively unreactive species. These reactions couple the odd-hydrogen and odd-nitrogen families in both the stratosphere¹ and the troposphere.² Two such gas-phase reactions are particularly important in the stratosphere. There, the reaction of HO₂ and NO₂ produces pernitric acid, which is an important temporary reservoir species. Also, the reaction of OH + NO₂ produces nitric acid, HONO₂, the dominant nitrogen reservoir species, and thus is largely responsible for the partitioning between NO_x and NO_y. When modeling odd-nitrogen chemistry, an overestimate of the rate of OH and NO₂ at stratospheric temperatures and pressures will result in an underestimate of the abundance of NO₂. Both reactions also have a role in the troposphere; HO₂ + NO₂ is a null reaction in the lower troposphere, where thermal decomposition is rapid, but OH + NO₂ is a major chain-termination reaction, leading to irreversible HO_x and NO_x loss and bypassing the ozone-production cycle.

Our understanding of reactive nitrogen partitioning relies on our understanding of the pivotal OH + NO₂ reaction. Both the rate constant and the reaction mechanism require attention in

this case: the rate constant because errors at standard temperature and pressure could introduce substantial errors in tropospheric chemical models, and the mechanism because minor reaction products could be directly significant, and could also complicate interpretation of the rate constant. The rate constant depends strongly on temperature and pressure. While it has been studied extensively at room temperature, a large uncertainty remains in the data at 760 Torr and above, and at lower temperatures. Most data and the JPL recommendation³ do not agree with either the IUPAC recommendation⁴ or the data of Forster et al.,⁵ obtained in high pressures of He. The disagreement is severe, reaching 50% at STP, and the implications for tropospheric ozone production models are similarly severe. Recent data from this lab⁶ and from Brown et al.⁷ have greatly improved our knowledge of the rate constant. Uncertainty in the mechanism remains significant at both low temperatures and high pressures.

OH + NO₂ Mechanism. The OH + NO₂ reaction has two possible reaction products: nitric acid, HONO₂, and peroxyxynitrous acid, HOONO:



In each case, the product is formed in an excited vibrational state, and collisionally stabilized by the chaperone gas, M. For HOONO to be significant in the atmosphere, it must be stable and β must be larger than a few percent. The potential energy surface for this family has been studied by several groups, and all are agreed on the critical point that HOONO lies lower in

[†] Part of the special issue "Harold Johnston Festschrift".

* Corresponding author.

[‡] Present address: Departments of Chemistry and Chemical Engineering, Carnegie Mellon University, Pittsburgh, PA 15213-3890.

energy than $\text{OH} + \text{NO}_2$, and is formed via a barrierless reaction.^{8,9} Furthermore, HOONO has been observed directly as a product of the photolysis of nitric acid in argon matrices,¹⁰ and both HOONO and the anion OONO^- , peroxyxynitrite, are known to be important species in solution, especially in the chemistry of living systems.¹¹ Yet peroxyxynitrous acid has never been observed in the gas phase. The only experiment to attempt to measure the branching of Reaction 1 obtained an 80% yield of nitric acid (α) and 0% yield of HOONO (β).¹² Consequently, we set out to directly measure the branching ratio of the reaction using Reaction Modulation Spectroscopy (RMS).

Quantification of the HOONO formation branching ratio is essential to answer several outstanding questions in the atmospheric chemistry of NO_x .

First, the presence of a secondary channel could explain the discrepancy between the low pressure and high-pressure data on the rate of $\text{OH} + \text{NO}_2$. The thermal lifetime of HOONO is expected to be quite short in comparison to HONO₂. As such, it is probable that experiments conducted at room temperature and on long time scales (milliseconds–seconds) would be unable to detect the formation of the peroxy isomer, as it would dissociate to reactants before the measurement took place. On the other hand, experiments conducted on short time scales (nanoseconds–milliseconds) would observe the loss of reactants before dissociation could occur. All of the experiments at high pressure are conducted on rapid time scales, while many experiments at lower pressures were carried out at longer time scales. Consequently, it is possible that these differing time scales could be biasing the data.

In addition, the presence of a peroxy intermediate could help to explain the formation of organic nitrates from reaction between RO_2 and NO . Current understanding of the potential energy surfaces involved indicates that direct formation of RONO_2 is impossible, due to large barriers to the entrance channel. However, there is a barrierless channel to form vibrationally excited ROONO , which certainly can decompose to form RO and NO_2 . On the other hand, some fraction of the ROONO could isomerize to RONO_2 . It should be noted that while the potential energy surface for the RO_2 reaction will be different from that for the HO_2 reaction, the general shape of the surface is conserved and the reaction mechanism should be similar.

Potential Energy Surface

In Figure 1, we present our own calculations on the HNO_3 potential energy surface, relative to $\text{OH} + \text{NO}_2$, calculated at B3LYP/6-31G**. The reaction $\text{OH} + \text{NO}_2$ can directly produce all stable isomers, but the reaction $\text{HO}_2 + \text{NO}$ cannot form HONO₂ due to a large barrier at the entrance channel. The energies of stable species shown here are in good agreement with other calculations. The transition states of the system are less well-known. The three transition states indicated in our results are labeled as TS1–3. TS1 is a hydrogen-transfer transition state that separates two normally indistinguishable isomers of nitric acid (HONO₂) which may be isotopically labeled. TS2 separates the two lowest-energy conformers of peroxyxynitrous acid (HOONO), cis-cis and trans-perp. Note that the barrier to direct isomerization between the equilibrium geometries of nitric acid and peroxyxynitrous acid is insurmountable without dissociation and is not shown in the figure. However, as the $\text{HO}-\text{NO}_2$ bond is stretched, the barrier to internal rotation drops rapidly. Dipole–induced dipole effects will be attractive over a wide range of the $\text{HO}-\text{NO}_2$ bond angle. If these effects eventually exceed the rotational barrier, there

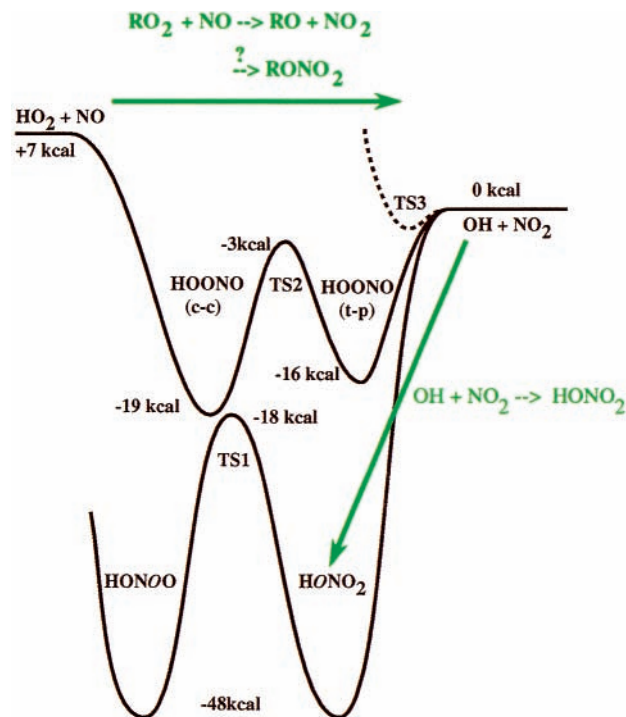


Figure 1. Species on the HNO_3 potential energy surface, relative to $\text{OH} + \text{NO}_2$ calculated at B3LYP/6-31G**. Radical fragments are on the wings of the figure, while stable molecules (nitric acid and peroxyxynitrous acid) occupy the middle. The reaction coordinate for the reaction $\text{HO}_2 + \text{NO} \rightarrow \text{OH} + \text{NO}_2$ proceeds from left to right in the figure. The reaction $\text{OH} + \text{NO}_2$ can directly produce all stable isomers. TS1 separates two normally indistinguishable isomers of nitric acid (HONO₂) that may be isotopically labeled. TS2 separates two conformers of peroxyxynitrous acid (HOONO), while TS3 is a postulated loose ($\text{HO}-\text{NO}_2$) isomerization transition state separating HOONO and HONO₂.

will be an isomerization transition state. We propose that at some configuration, labeled TS3 here, the barrier to internal rotation lies below that of dissociation, and the species may rotate from an HOONO conformation to an HONO₂ conformation, and then relax to the bottom of the well. Density functional calculations at such interatomic distances are not accurate. On the other hand, of the affordable levels of theory, only DFT calculations are able to deal with the presence of the multiple electronegative atoms present in the HNO_3 family.¹³ Our B3LYP calculations locate such a loose rotational transition state, but we cannot claim knowledge of its exact position or energy, merely that some such transition state is likely to exist. If such a low-energy transition state does exist, vibrationally excited HOONO could isomerize directly to HONO₂. It is thus possible that HOONO produced by Reaction 1b could isomerize before being quenched. This would substantially complicate the reaction dynamics.

Recent dynamics calculations performed on the HNO_3 surface have produced conflicting results regarding the importance of the peroxy channel. Golden and Smith¹⁴ conducted Hindered-Gorin RRKM calculations that predict a significant branching ratio of the peroxyxynitrous product. These results yield a lifetime for HOONO of seconds or longer under almost all atmospheric conditions. On the other hand, Matheu and Green¹⁵ applied an extensive master equation treatment to the problem, and conclude that branching to form HOONO is insignificant under all atmospherically relevant conditions, and only becomes significant at thousands of Torr. Their result can thus explain the deviation of the very high-pressure data of Forster et al.,⁵ but not the discrepancy at STP. Neither study confronts the

possibility of isomerization of the vibrationally excited intermediate. Obviously, more experimental data are needed.

The potential energy surface for the RO₂ + NO reaction is similar in shape to that shown here for HO₂ + NO. The transition states on that surface are also largely unidentified, but for small R, they are qualitatively the same as for the HO₂ case. The barrier to direct formation of RONO₂ is very high, and the direct isomerization barrier lies above dissociation at the equilibrium geometry. These high barriers confound explanations of the observed RONO₂ products from reactions of RO₂ + NO; the product cannot be formed directly, nor can it be formed through a direct isomerization. Note that, unlike the HNO₃ system, the density of states of the vibrationally excited ROONO product is closer to the density of RONO₂, and becomes closer still as R increases in size, increasing the probability of ROONO formation. Isomerization from ROONO to RONO₂ may explain the observation that the yield of RONO₂ increases with R.¹⁶ On the other hand, it is hard to extract much information about RO₂ + NO from experimental observations of OH + NO₂: not only are we losing many reactive modes by substituting H for R, but we are approaching the stable molecules along a different reaction coordinate. Thus, even a lack of observed HOONO from OH + NO₂ does not preclude the possibility of ROONO formation from RO₂ + NO.

Experimental Section

Our high-pressure flow system has been extensively described in the literature. The fluid dynamics of the “core flow” conditions have been described analytically,¹⁷ and we have obtained high-accuracy results from 2 to 600 Torr (e.g., ref 18) and from 175 to 400 K (e.g., ref 19), including work on the OH + NO₂ reaction [ref 18, ref 6]. Reactions between two radical species can be problematic for many experiments. The HPFS is designed to study radical–molecule reactions, aided by the careful control of radical production and the isolation of the reaction zone from the wall. Therefore, homogeneous and heterogeneous chemical interferences are largely eliminated. The microwave discharge sidearm source allows control over the character of the radical plume and the concentration of the radicals without disturbing the bulk flow down the tube, and our wall-less environment solves the loss problems associated with the radical species. The experiments described here are reaction product studies, conducted using Reaction Modulation Spectroscopy (RMS²⁰). In particular, a radical is injected into a plume of NO₂, and we simultaneously monitor removal of NO₂ and appearance of any reaction products using Fourier transform infrared spectroscopy. The RMS method affords us a very high signal-to-noise ratio free of background interference, and enables us to use careful mass-balance to investigate the branching ratios of the reactions studied.

FTIR Nonlinearity. Our experimental design requires that we use very large concentrations of NO₂ (up to 10¹⁵ molecules/cm³), and the results are based on measuring relatively small changes in these large concentrations. This presents two challenges: first, we must be certain that, aside from the chemistry, nothing significantly changes the NO₂ concentration; second, quantitative analysis of the low-resolution FTIR data is difficult because Beer’s law does not hold directly. The first issue is addressed by very carefully controlling all flows in the system, as well as actively controlling the system pressure. We verify that NO₂ changes that are not correlated with the chemical modulation are much smaller (typically 1% or less) than those driven by the chemistry. The second issue requires careful

treatment of the IR analysis. In particular, we model all aspects of the IR spectroscopy as part of the quantitative analysis. We generate a synthetic high-resolution spectrum of NO₂ from the known line-by-line spectrum for a specific pressure and temperature and calculate the high-resolution transmittance spectrum for a given NO₂ column. This transmittance spectrum is then degraded to our instrument resolution (0.5 cm⁻¹), including self-apodization, producing a synthetic spectrum that is compared directly with the observed data. This process is iterated until the synthetic spectrum and the data match. To model the small difference (which nonetheless produces an IR signature with high signal-to-noise), we must explicitly model the change in transmittance at high resolution by generating spectra for both values of the NO₂ column, then degrade each high-resolution transmittance spectrum and take the ratio of the resulting low-resolution spectra. This exactly matches the radiative transfer producing our data and generates a low-resolution spectrum that is linearized about the nearly constant NO₂ column present in the experiment.

HO₂ + NO₂. We will first consider the reaction of the hydroperoxy radical with nitrogen dioxide to produce the reservoir species pernitric acid. There are two possible reaction channels:



However, since 1977, it has been known that Reaction 2a is the primary channel under atmospheric conditions. Indeed, Reaction 2a was used in the first experiments to detect the existence of pernitric acid.²¹ Recently, the importance of pernitric acid as an intermediate in stratospheric chemistry and in the urban troposphere has led to much interest in its chemistry and its spectroscopy. If even a minor fraction of Reaction 2 were to proceed through Reaction 2b, this would be a significant source of nitrous acid, HONO. Not surprisingly, experiments carried out at high pressure confirm that no HONO is formed.²² However, the only feasible mechanism for the H-atom transfer involved would be through vibrationally excited HOONO₂. The question thus becomes where in energy the H-atom transfer transition state lies relative to the reactants.

We present a simple, two-step gas-phase synthesis of HOONO₂ which produces a clean spectrum with no interfering absorbers. Our experiment was conducted at 120 Torr. A large excess of NO₂ (10% in He, Scott Specialty Gases) is injected through a loop injector far upstream (3 m) of the reaction zone and introduced into the center of a 10 m/s flow of N₂ carrier gas. Hydrogen gas is passed through a microwave discharge in a sidearm, and mixed with a large excess of O₂, quickly and efficiently producing HO₂ radicals that are then injected into the center of the bulk flow:



The HO₂ reacts rapidly with the NO₂ to form HOONO₂. The flow of hydrogen gas is modulated, and FTIR scans are recorded with the hydrogen both on and off. Measurements are made well before the plume encounters the tube wall, ensuring wall-less conditions. The resultant spectrum is shown in Figure 2.

As can be seen, there are no features in the spectrum which can be attributed to HONO. As this experiment is conducted well into the falloff region for Reaction 2a (the center of the falloff curve is at approximately one atmosphere), and thus the

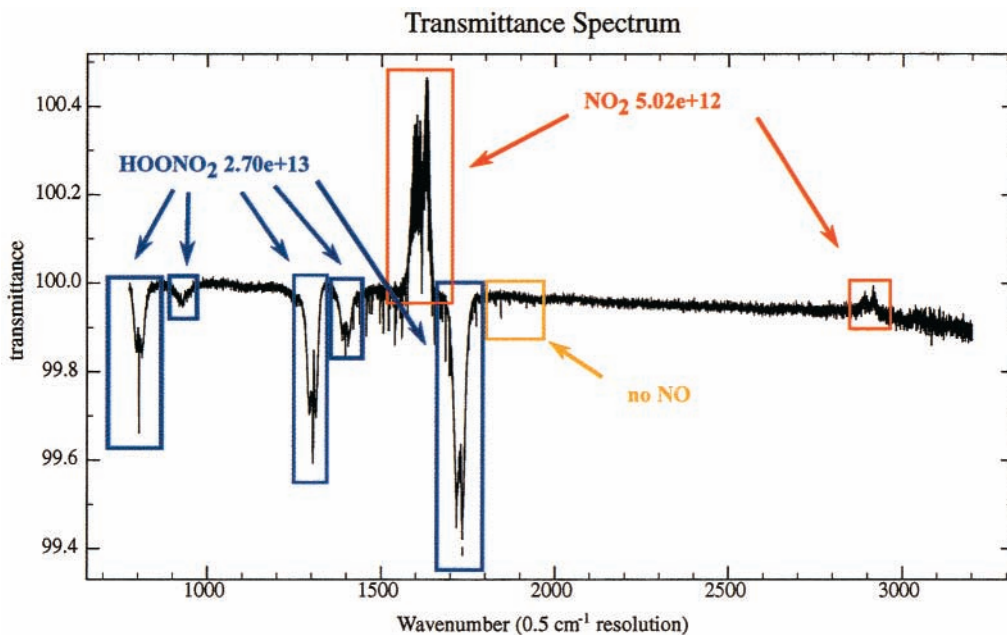


Figure 2. RMS results for the reaction of $\text{HO}_2 + \text{NO}_2 \rightarrow \text{HOONO}_2$. Products appear below the baseline as optical depth increases, and reactants consumed during the reaction appear above the baseline as optical depth decreases. Resolution is 0.5 cm^{-1} .

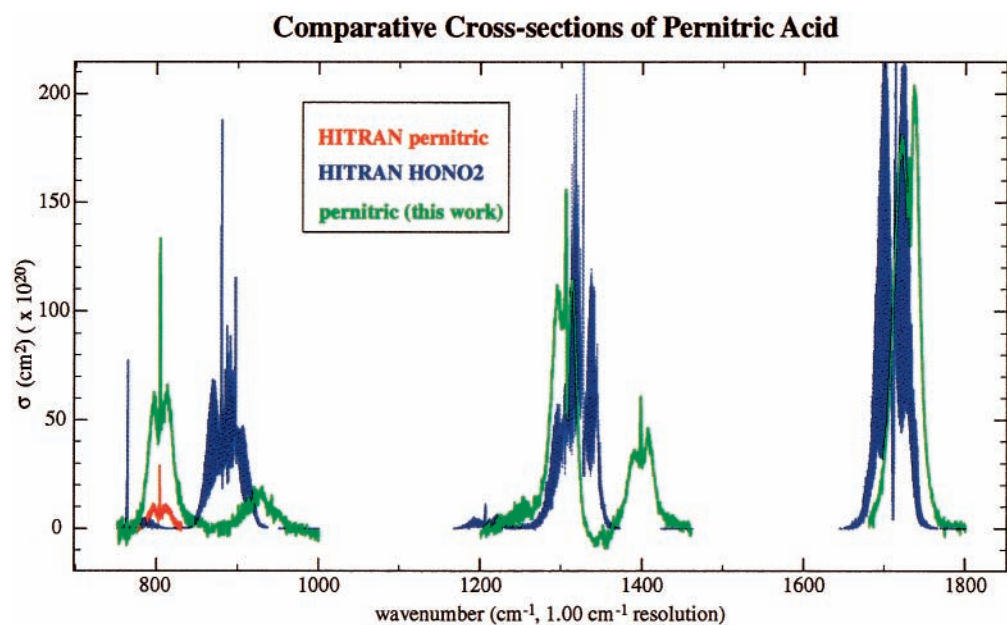


Figure 3. The red plot is the HITRAN cross-section for pernitric acid. Shown in green is the cross-section for pernitric acid extracted from our RMS experiment. In blue is the HITRAN cross-section for the comparable features of nitric acid, showing values similar to the extracted values for pernitric, but radically different from the HITRAN pernitric.

vibrationally excited HOONO_2 would have the opportunity to completely sample the phase space, the lack of HONO is strong evidence that the hydrogen transfer transition state is inaccessible.

We monitor the change in concentration of the NO_2 and HOONO_2 species via FTIR. In this system, we see an additional power of the RMS technique: in a clean and simple reaction such as this, we can use mass balance to determine the cross-section of a species which is otherwise difficult to synthesize. As can be seen in the sample spectrum, the extracted $[\text{HOONO}_2]$ using the HITRAN cross-section is a factor of 4–5 too high to be explained by the depletion of NO_2 . As there are no other features in the RMS spectrum, we can be certain that there are no species missing from our mass balance equation to account

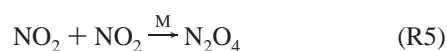
for the missing nitrogen, and we conclude that there is a significant problem with the integrated cross-section of the pernitric acid band. We also present in Figure 3 a plot of the cross-sections of pernitric acid given by HITRAN, pernitric acid inferred from the change in NO_2 concentration in our experiment, and nitric acid over the same region. Given the comparable structures and ab initio band intensities between HONO_2 and HOONO_2 , we expect comparable bands for the two compounds to have similar integrated cross-sections. In fact, the value for the integrated cross-section in the HITRAN database, taken from an experiment by Massie et al.,²³ differs by a factor of 5 from other values in the literature. The cross-section presented in Figure 3 agrees to within 10% with the value given in May and Friedl²⁴ for all features except the band

at 1728 cm⁻¹. This is an excellent indicator not only of the quality of the spectrum, but also of the accuracy of the extracted NO₂ concentration. Our cross-section for the 803 cm⁻¹ band is 10% higher than the value of ref 24 obtained at 220 K; this is likely a result of the known presence of hot bands at higher temperatures.²⁵

OH + NO₂. The instrumentation and procedure are similar to the HO₂ + NO₂ experiment described above. Rather than injecting H₂ and O₂ in the sidearm, we pass H₂ through the microwave, and inject the H atoms directly into the center of the flow. Hydroxyl radicals are rapidly generated via



and the concentration of OH is monitored using laser-induced fluorescence (LIF) at 5 locations along the flow tube. The OH produced then proceeds to react with the excess NO₂ according to Reactions 1a and 1b. At low temperatures, the analysis is complicated by the dimerization of NO₂:



The flow of hydrogen gas is again modulated, and concentrations of NO₂, NO, and HONO₂ are monitored by FTIR absorption using RMS.

Results

Shown in Figure 4 are our RMS spectra for the OH + NO₂ reaction under several different conditions. The resolution in all spectra is 0.5 cm⁻¹. The first panel is a product study at 60 Torr and room temperature, showing a nitrogen mass balance of 96 ± 3%, α of 87 ± 2.0%, and β of 0 ± 3.0%. The uncertainties are precisions, and do not include uncertainties in the individual cross-sections. As there is no visible feature of HOONO, and the gas-phase spectrum is unknown, we are unable to perform a correlation analysis directly. The uncertainty in β is obtained from the signal-to-noise ratio of the nearby nitric acid peaks, which are expected to be of comparable strength. Similarly, Figure 4b shows a run at 160 Torr and room temperature, giving a nitrogen mass balance of 96.5 ± 3.5%, α of 92 ± 3.5%, and β of 0 ± 4.1%. In neither case are there any spectral features other than NO₂, HONO₂, and NO. In all experiments conducted without formation of N₂O₄, we account for 96% of the NO₂ consumed by the reaction using only NO and HONO₂. We can calculate α, the branching ratio to nitric acid, by dividing the concentration of nitric acid by the difference in concentration between NO₂ and NO; the derivation of this formula is discussed below. The average α obtained from the room-temperature experiment is 91 ± 5%, independent of pressure, and β, the branching ratio to peroxyxynitrous acid, is 0 ± 3.5%. Figure 4c shows a spectrum taken at 375 Torr and 230K. There are two new spectral features in evidence, but these are each attributed to N₂O₄, formed from the NO₂ at low temperatures. If the features of HOONO are of comparable strength to those of HONO₂, as expected, then the absence of features in these spectra suggests concentrations of significantly less than 1 × 10¹² molecules/cm³; our detection limit for HONO₂ is approximately 5 × 10¹¹ molecules/cm³.

Literature Comparison

There are three reports in the literature with which we can quantitatively compare our results for the formation of HOONO from the reaction of OH + NO₂. Two of these (Golden and Smith (ref 14), Matheu and Green (ref 15)) are calculations

performed on a potential energy surface with the assistance of chemical kinetic data, while the third, Burkholder et al. (ref 12), is an experiment designed to investigate the formation directly. Our results agree well with the Burkholder experiment, which uses the same reaction sequence as our study. Their experiment measured the ratio of nitric acid to NO in order to obtain a branching ratio; as will be discussed below, our experiment allows for a more direct measure of α. They observed HONO₂ formation with α = 0.8, independent of temperature and pressure, but saw no evidence for HOONO or any other products. Our results agree with the Burkholder experiment in that we also see no evidence for HOONO formation under any conditions studied, but our experiment allows for a significant reduction in the uncertainty in α and β. Golden and Smith (ref 14) predict a significant branching ratio to form HOONO under all conditions, which we do not observe. Furthermore, the Golden and Smith calculations predict a value of β approaching 30% at STP, increasing with increasing pressure and decreasing temperature. While this result would indeed be powerful in explaining the rate constant discrepancy at STP, we do not observe the predicted β of nearly 20% at 100 Torr. The RRKM calculations also predict lifetimes for the HOONO molecule ranging from 0.01 s at STP to 100 s under stratospheric conditions. The Matheu and Green (ref 15) calculations, on the other hand, predict no HOONO formation under any low-pressure conditions. At STP, Matheu and Green predict only a 1% value for β, and the branching at room temperature only reaches 10% at approximately 20000 Torr. Our result does not constrain their calculations, but those calculations cannot explain the apparent discrepancy in rate constant data at STP.

Discussion

Our data are only the second direct measurement of the branching ratio of the reaction of OH and NO₂. The Burkholder et al. experiment¹² was conducted using the same series of reactions, and the reported branching ratio was obtained by comparing the amount of nitric acid produced to the amount of NO produced. We monitor the concentrations of both reactants and products, allowing us the additional constraint of NO₂ concentrations. We account for 96% of the NO₂ consumed by the reaction using only NO and HONO₂. Unlike the Burkholder branching ratio, we can obtain a direct measure by subtracting the measured NO production from the measured NO₂ consumption. We calculate α by dividing the HONO₂ concentration by the consumed amount of NO₂ unaccounted for by NO production; the remaining NO₂ consumption is certainly due to reaction with OH, and thus the remainder is compared to the amount of HONO₂ produced to obtain branching ratios.

$$\alpha = \frac{[\text{HONO}_2]}{[\text{NO}_2] - [\text{NO}]} \quad (1)$$

In these experiments, the calculated α is 91%, on average. It should be stressed that this branching ratio is quite probably unity, given the uncertainty in the measurements and associated cross-sections, and the lack of spectral evidence of any other species. Note that our experiment, like the Burkholder experiment, consistently produces a ratio of nitric acid to NO of less than one. The ratio is highly pressure sensitive, and also dependent on the flow rates of the radical source, but in all cases ranges from 50% to 90%. With the addition of the NO₂ concentration, however, we are not forced to consider this ratio as our value of α. As was the case in Burkholder's experiments, this inequality is probably not due to the formation of HOONO,

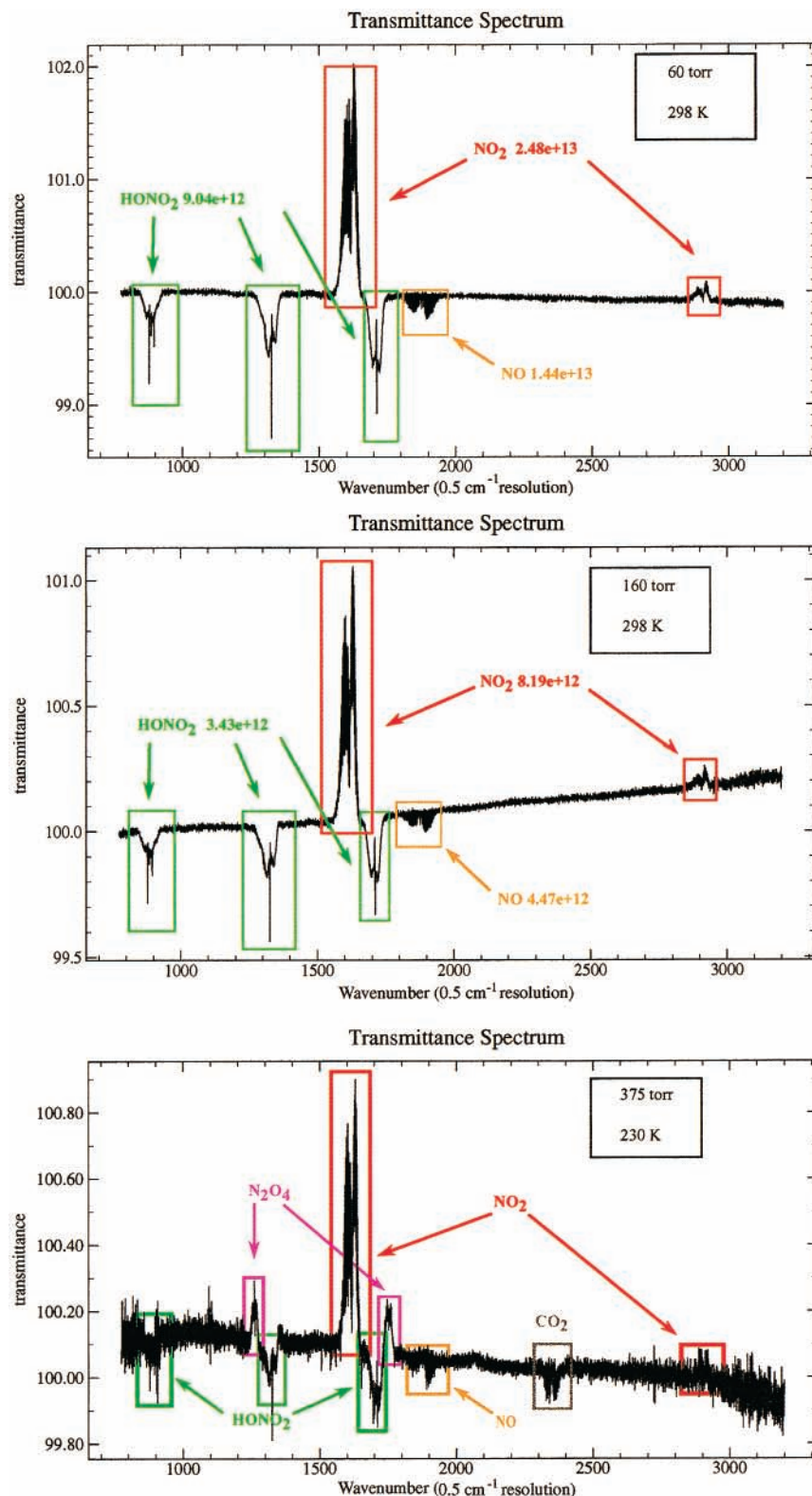


Figure 4. Three sample RMS spectra for the reaction of OH + NO₂. Measured reactant and product concentrations are shown for the room-temperature spectra. Resolution is 0.5 cm^{-1} . The only products observed are NO and HONO₂. The third panel shows an RMS experiment at 375 Torr and 230 K. New features are N₂O₄, and no new products are observed.

which we would observe in the IR. Rather, we believe that it is the result of diffusion-limited gas-phase chemistry invisible to the IR that consumes the OH produced in the titration portion of the reaction. When the initial titration takes place in the center of the flow tube, a plume of highly concentrated OH is produced that is as likely to self-react as to react with NO₂, at least until diffusion proceeds sufficiently to mix the plume with the

surrounding NO₂. Nonetheless, since such reactions do not consume NO₂ or produce HONO₂, we can exclude them from consideration in the branching; the self-reaction of OH represents a loss of potentially reactive radicals from the first step of our reaction sequence to the second, but does not hinder our branching ratio measurement so long as sufficient OH survives to obtain a good signal-to-noise ratio in the HONO₂ features.

We see no evidence for the formation of pernitrous acid at room temperature and low pressure. Furthermore, our results at low temperature and higher pressure show no unexplained spectral features. While we have yet to reach tropospheric pressures, or the temperatures of the lower stratospheric winter, this investigation presents evidence that the branching ratio of the reaction remains at least 90% in favor of nitric acid under the conditions studied. We plan to extend our study to below 200 K and above 500 Torr, but the current results do not support the possibility of pernitrous acid playing a significant role in the partitioning of nitrogen in the atmosphere. However, the results under these conditions do not contradict the proposal that this intermediate could explain the discrepancy between high- and low-pressure measurements of the OH + NO₂ rate constant. The great discrepancy between these studies begins at pressures above those observed in this experiment.

The implications of any HOONO formation for atmospheric chemistry would be substantial were this channel to exist. Were it to contribute to the apparent discrepancy between very high-pressure data and other data, those lower-pressure data would give the experimental rate constant for reaction R4a, the rate of HONO₂ formation. The high-pressure rate constants are measured on a rapid enough time scale that any HOONO formed would be observed as lost reactants. These then would be a convolution of the rate constants to form nitric acid and peroxyxynitrous acid. On the other hand, data taken at lower pressures are either blind to HOONO formation because of the experimental time scale or there is not significant HOONO formation at all. If the time scale is the limiting factor, then any HOONO formed under atmospheric conditions will also decompose rapidly, regenerating the OH and NO₂ radicals. Thus, OH + NO₂ → HOONO would be a null reaction on any significant atmospheric time scale, and the low-pressure data are the correct values to use in atmospheric chemistry models. Our results do not provide a conclusive answer on this point, but they appear to be inconsistent with Golden and Smith¹⁴ and consistent with Matheu and Green¹⁵ in that we see no HOONO formation under our experimental conditions. The results of Matheu and Green, however, cannot explain the discrepancy in rate data at STP, so this issue needs more input.

Of great utility in explaining this dilemma is the companion paper by Donahue et al.,²⁶ which performs an extensive analysis of the rate data, including the rate of ¹⁸OH + NO₂ up to 150 Torr at room temperature. The isotopic scrambling reaction ¹⁸OH + NO₂ → HO + ¹⁸ONO is mediated only by HONO₂. Consequently, the disappearance rate constant of ¹⁸OH can be used to deduce the formation rate constant of HONO₂ as a function of pressure.²⁷ The constraints provided by the pressure dependence of the ¹⁸OH + NO₂ and OH + NO₂ reactions are sufficient to permit a purely kinetic determination of the branching between HOONO and HONO₂ formation.²⁶ The results are within 20% of the values of Golden and Smith (ref 14).

As the results of Golden and Smith and Donahue et al. (ref 26) are quantitatively in agreement and almost entirely independent, it is hard to explain why this RMS experiment failed to observe any HOONO. It is possible that peroxyxynitrous acid is formed under the studied conditions, but is not observed in the IR. There are a handful of explanations of how this could be true. First, the HOONO thermal lifetime could be less than 0.1 s at the temperatures observed, and the product dissociates before being observed. However, this is hard to account for given the potential energy surfaces believed to be involved. Another possibility is that the HOONO product is formed in a distribution among several conformers, thus decreasing the

cross-section of any one product species. Indeed, we have identified three conformers with similar heats of formation and isomerization barriers nearly as high as the OH + NO₂ energy. It is also conceivable that the IR cross-section of the individual peaks of the HOONO spectrum are significantly weaker than the corresponding features of nitric acid. Finally, both kinetic results (Golden and Smith and Donahue et al.) are constrained at high pressure by the high-pressure data of Fulle,²⁸ which are approximately 40% higher than the measured rate for vibrational deactivation of OH by NO₂.²⁹ If this latter result is more accurate, the HOONO formation branching ratio under our conditions would also be 40% lower. The most likely explanation is that these factors combine to render a modest branching ratio (less than 20%) distributed among several species and thus many absorption features collectively below our detection threshold.

Conclusions

Our Reaction Modulation Spectroscopy experiments support the conclusion that the secondary product channel of the reaction of HO₂ + NO₂ is negligible, as the hydrogen transfer transition state which would yield HONO + O₂ is inaccessible. In addition, our experiments provide no direct evidence of peroxyxynitrous acid formation from OH + NO₂ under stratospheric conditions, and suggest that HOONO will not form in any significant amount under any sub-atmospheric pressure. We obtain branching ratios to form nitric acid of unity, within experimental uncertainty. However, there is evidence that HOONO formation could explain the discrepancy between low- and high-pressure rate constant measurements of the reaction of OH + NO₂. Therefore, while our experiment helps to constrain the branching ratio of the HOONO channel, further experiments at lower temperatures and higher pressures are required in order to conclusively establish or rule out the role of HOONO.

Acknowledgment. This work was funded by grants from NSF (grant number 997792) and US EPA (grant number R825258010).

References and Notes

- (1) Johnston, H. Reduction of stratospheric ozone by nitrogen oxide catalysts from supersonic transport exhaust. *Science* **1971**, *173*, 517.
- (2) Logan, J. A.; Prather, M. J.; Wofsy, S. C.; McElroy, M. B. Tropospheric chemistry: a global perspective. *J. Geophys. Res.* **1981**, *86*, 7210.
- (3) DeMore, W. B.; Friedl, R. R.; Golden, D. M.; Hampson, R. F.; Huie, R. E.; Kolb, C. E.; Kurylo, M. J.; Molina, M. J.; Moortgat, G. K.; Ravishankara, A. R.; Sander, S. P. Chemical kinetics and photochemical data for use in stratospheric modeling. Technical Report 00-3, Jet Propulsion Laboratory, 2000.
- (4) Atkinson, R.; Baulch, D. L.; Cox, R. A., Jr.; Hampson, R. F.; Kerr, J. A.; Rossi, M. J.; Troe, J. Evaluated kinetic and photochemical data for atmospheric chemistry. supplement VI. IUPAC subcommittee on gas kinetic data evaluation for atmospheric chemistry. *J. Phys. Chem. Ref. Data* **1997**, *26*, 1329.
- (5) Forster, R.; Frost, M.; Fulle, D.; Hamann, H. F.; Hippler, H.; Schlegel, A.; Troe, J. High-pressure range of the addition of HO to HO, NO, NO₂, and CO: I. Saturated laser induced fluorescence measurements at 298 K. *J. Chem. Phys.* **1995**, *103*, 2949.
- (6) Dransfield, T. J.; Perkins, K. K.; Donahue, N. M.; Anderson, J. G.; Sprengenther, M. M.; Demerjian, K. L. Temperature and pressure dependent kinetics of the gas-phase reaction of the hydroxyl radical with nitrogen dioxide. *Geophys. Res. Lett.* **1999**, *26*, 687.
- (7) Brown, S. S.; Talukdar, R. K.; Ravishankara, A. R. Rate constants for the reaction OH + NO₂ + M → HNO₃ under atmospheric conditions reaction. *Chem. Phys. Lett.* **1999**, *299*, 277.
- (8) McGrath, J. P.; Rowland, F. S. Determination of the barriers to internal rotation in ONOOX (X = H, Cl) and characterization of the minimum energy conformers. *J. Phys. Chem.* **1994**, *98*, 1061.
- (9) Chakraborty, D.; Park, J.; Lin, M. C. Theoretical study of the OH + NO₂ reaction: formation of nitric acid and the hydroperoxy radical. *Chem. Phys. Lett.* **1998**, *231*, 39.
- (10) Lo, W.-J.; Lee, Y. P. Infrared absorption of cis-cis peroxyxynitrous acid (HOONO) in solid argon. *J. Chem. Phys.* **1994**, *101*, 5494.

- (11) Ischiropoulos, H. The second international conference on the biology and chemistry of peroxyxynitrite—foreword. *Nitric Oxide—Biology and Chemistry* **1999**, *3*, 1.
- (12) Burkholder, J. B.; Hammer, P. D.; Howard, C. J. Product analysis of the $\text{OH} + \text{NO}_2 + \text{M}$ reaction. *J. Phys. Chem.* **1987**, *91*, 2136.
- (13) Jursic, B. A study of nitrogen oxides by using density functional theory and their comparison with ab initio and experimental data. *Int. J. Quantum Chem.* **1996**, *58*, 41.
- (14) Golden, D. M.; Smith, G. P. Reaction of $\text{OH} + \text{NO}_2 + \text{M}$: A new view. *J. Phys. Chem.* **2000**, *104*, 3991.
- (15) Matheu, D. M.; Green, W. H. A priori falloff analysis for $\text{OH} + \text{NO}_2$. *Int. J. Chem. Kinet.* **2000**, *32*, 245.
- (16) Carter, W. P. L.; Atkinson, R. Alkyl nitrate formation from the atmospheric photooxidation of alkanes; a revised estimation method. *J. Atmos. Chem.* **1989**, *8*, 165.
- (17) Donahue, N. M.; Clarke, J. S.; Demerjian, K. L.; Anderson, J. G. Free radical kinetics at high pressure: A mathematical analysis of the flow reactor. *J. Phys. Chem.* **1996**, *100*, 5821.
- (18) Donahue, N. M.; Dubey, M. K.; Mohrschladt, R.; Demerjian, K. L.; Anderson, J. G. A high-pressure flow study of the reactions $\text{OH} + \text{NO}_x \rightarrow \text{HONO}_x$: Errors in the falloff region. *J. Geophys. Res.* **1997**, *102*, 6159.
- (19) Clarke, J. S.; Kroll, J. H.; Donahue, N. M.; Anderson, J. G. Testing frontier orbital control: $\text{OH} +$ ethane, propane, and cyclopropane from 180 to 360 K. *J. Phys. Chem.* **1998**, *102*, 9847.
- (20) Donahue, N. M.; Demerjian, K. L.; Anderson, J. G. Reaction modulation spectroscopy: a new approach to quantifying reaction mechanisms. *J. Phys. Chem.* **1996**, *100*, 17855.
- (21) Niki, H.; Maker, P. D.; Savage, C. M.; Breitenbach, L. P. Fourier transform IR spectroscopic observation of pernitric acid formed via $\text{HO}_2 + \text{NO}_2 \rightarrow \text{HOONO}_2$. *Chem. Phys. Lett.* **1977**, *45*, 564.
- (22) Tyndall, G. S.; Orlando, J. J.; Calvert, J. G. Upper limit for the rate constant for the reaction $\text{HO}_2 + \text{NO}_2 \rightarrow \text{HONO} + \text{O}_2$. *Environ. Sci. Technol.* **1995**, *29*, 202.
- (23) Massie, S. T.; Goldman, A.; Murcray, D. G.; Gille, J. C. Approximate absorption cross sections of F12, F11, ClONO_2 , N_2O_5 , HNO_3 , CCl_4 , F21, F113, F114, and HNO_4 . *Appl. Opt.* **1985**, *24*, 3426.
- (24) May, R. M.; Friedl, R. R. Integrated band intensities of HO_2NO_2 at 220 k. *J. Quant. Spectrosc. Radiat. Transfer* **1993**, *50*, 257.
- (25) Friedl, R. R.; May, R. M.; Duxbury, G. The ν_6 , ν_7 , ν_8 , and ν_{10} bands of HO_2NO_2 . *J. Mol. Spectrosc.* **1994**, *165*, 481.
- (26) Donahue, N. M.; Dubey, M. K.; Mohrschladt, R.; Dransfield, T. J.; Anderson, J. G. Constraining the mechanism of $\text{OH} + \text{NO}_2$ using isotopically labeled reactants: experimental evidence for HOONO formation. *J. Phys. Chem. A*, this issue.
- (27) Greenblatt, G. D.; Howard, C. J. Oxygen atom exchange in the interaction of (18) OH with several small molecules. *J. Phys. Chem.* **1989**, *93*, 1035.
- (28) Fulle, D.; Hamann, H. F.; Hippler, H.; Troe, J. Temperature and pressure dependence of the addition reactions of HO to NO and to NO_2 . IV. saturated laser-induced fluorescence measurements up to 1400 bar. *J. Chem. Phys.* **1998**, *108*, 5391.
- (29) Smith, I. W. M.; Williams, M. D. Vibrational relaxation of $\text{OH}(v=1)$ and $\text{OD}(v=1)$ by HNO_3 , DNO_3 , H_2O , NO and NO_2 . *J. Chem. Soc. Faraday Trans.* **1985**, *81*, 1849.